Grid Application and Controls Development for Medium-Voltage SiC-Based Grid Interconnects

Preprint

Akanksha Singh, Xiangqi Zhu, Barry Mather, and Firehiwot Gurara

National Renewable Energy Laboratory

Presented at the IEEE Energy Conversion Congress & Exposition (ECCE)
October 11–15, 2020

NREL is a national laboratory of the U.S. Department of Energy
Office of Energy Efficiency & Renewable Energy
Operated by the Alliance for Sustainable Energy, LLC

This report is available at no cost from the National Renewable Energy Laboratory (NREL) at www.nrel.gov/publications.

Contract No. DE-AC36-08GO28308

Conference Paper
NREL/CP-5D00-75828
October 2020

Grid Application and Controls Development for Medium-Voltage SiC-Based Grid Interconnects

Preprint

Akanksha Singh, Xiangqi Zhu, Barry Mather, and Firehiwot Gurara

National Renewable Energy Laboratory

Suggested Citation
Singh, Akanksha, Xiangqi Zhu, Barry Mather, and Firehiwot Gurara. 2020. *Grid Application and Controls Development for Medium-Voltage SiC-Based Grid Interconnects: Preprint*. Golden, CO: National Renewable Energy Laboratory. NREL/CP-5D00-75828. https://www.nrel.gov/docs/fy21osti/75828.pdf.

NREL is a national laboratory of the U.S. Department of Energy
Office of Energy Efficiency & Renewable Energy
Operated by the Alliance for Sustainable Energy, LLC

This report is available at no cost from the National Renewable Energy Laboratory (NREL) at www.nrel.gov/publications.

Contract No. DE-AC36-08GO28308

Conference Paper
NREL/CP-5D00-75828
October 2020

National Renewable Energy Laboratory
15013 Denver West Parkway
Golden, CO 80401
303-275-3000 • www.nrel.gov

NOTICE

This work was authored in part by the National Renewable Energy Laboratory, operated by Alliance for Sustainable Energy, LLC, for the U.S. Department of Energy (DOE) under Contract No. DE-AC36-08GO28308. Funding provided by U.S. Department of Energy Office of Energy Efficiency and Renewable Energy Advanced Manufacturing Office. The views expressed herein do not necessarily represent the views of the DOE or the U.S. Government.

Cover Photos by Dennis Schroeder: (clockwise, left to right) NREL 51934, NREL 45897, NREL 42160, NREL 45891, NREL 48097, NREL 46526.

Grid Application and Controls Development for Medium-Voltage SiC-Based Grid Interconnects

Akanksha Singh, Xiangqi Zhu, Barry Mather, and Firehiwot Gurara
Power Systems Engineering Center
National Renewable Energy Laboratory
Golden, CO, USA
akanksha.singh@nrel.gov, xiangqi.zhu@nrel.gov, barry.mather@nrel.gov, fwg24@cornell.edu

***Abstract*— This paper studies, the grid-interconnection requirements of directly connected medium-voltage (MV) Silicon Carbide-based (SiC-based) converters and details the necessary control implementations. These power electronic converters follow the interconnection standard IEEE 1547-2018, but can also have additional controls supported by the microgrid standards in IEEE 2030.7, which is demonstrated in this work. Additionally, this paper defines the grid applications realized by these directly connected medium-voltage power electronic converters at the distribution scale and demonstrates results. The controls for the studied grid applications are then developed and implemented on the controller. The paper also includes details of the control algorithm development and validations of the control algorithm through hardware-in-the-loop results.**

Keywords—distribution system, grid application, back-to-back converter, controller development

I. Introduction

With the increasing commercial availability of high-quality, and reliable Silicon Carbide (SiC) devices that can operate at voltages relevant to medium-voltage distribution utility applications [1], it is critical to develop a technical pathway for such applications to ensure the successful, widespread use of medium-voltage SiC devices and modules. The adoption of medium-voltage SiC-based power electronics in the electric grid would provide an important tool for the efforts in grid modernization. The grid-connected power converters are used in medium-voltage distribution grids for myriad applications such as, solid-state circuit breakers, fault-current limiter, and power conditioning systems. [2] – [5]. Additionally, the increasing penetration of renewable energy sources into the power grid has resulted in increased medium-voltage power converters as interfaces to these energy resources [6] – [8]. It is estimated that, approximately 99% of the power generated by the present photovoltaic (PV) power plants in the world is being injected into medium-voltage grids [9] – [12]. Fig. 1 shows the potential range of directly-connected medium-voltage power electronic converters, including: medium-voltage to low-voltage conversion (i.e. a solid-state transformer); medium-voltage to DC conversion to easily integrate inherently DC systems such as photovoltaics (PV), battery systems, and electric vehicles; and medium-voltage to medium-voltage back-to-back (MVB2B) converters (highlighted in yellow and the focus application of this paper), which connect portions of grids together and allow full asynchronous power flow control between intertied distribution systems.

In this paper, Section II presents the study of multiple standards that are used to identify and implement necessary grid support controls required to enable the direct connection of medium-voltage SiC-based back-to-back ac power converters for distributed energy resources (DERs) to the grid, microgrid to microgrid connection, and microgrid to grid interconnection, including IEEE 1547-2018, IEEE 2030.7. Section III presents analysis for grid applications development. This section presents capabilities enabled by a directly connected MVB2B converter and compares them to a system with traditional components. This also helps quantify the benefits of having these solid-state interconnects in the grid through grid voltage support, reactive power compensation, etc. Section IV presents a detailed explanation of the development of controls for the applications developed in Section III. Section IV also includes the implementation and results from the evaluation of the developed controls on a 500 kW, 13.8 kV back-to-back converter through a controller-hardware-in-the-loop (CHIL) setup. Finally, Section V presents the conclusion and the focus of future work.

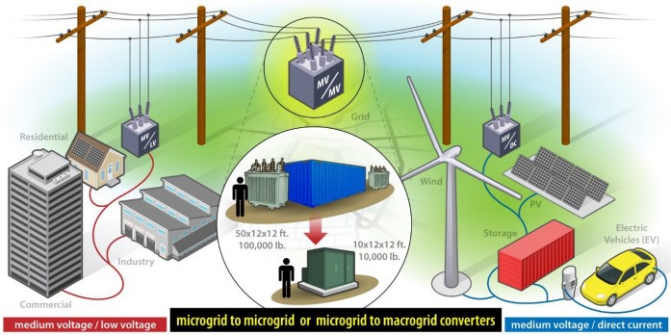

Fig. 1. Grid application examples of directly connected medium-voltage power electronic converters including a medium-voltage/medium-voltage intertie.

This work was authored by Alliance for Sustainable Energy, LLC, the manager and operator of the National Renewable Energy Laboratory for the U.S. Department of Energy (DOE) under Contract No. DE-AC36-08GO28308. Funding provided by U.S. Department of Energy Office of Energy Efficiency and Renewable Energy Advanced Manufacturing Office. The views expressed in the article do not necessarily represent the views of the DOE or the U.S. Government. The U.S. Government retains and the publisher, by accepting the article for publication, acknowledges that the U.S. Government retains a nonexclusive, paid-up, irrevocable, worldwide license to publish or reproduce the published form of this work, or allow others to do so, for U.S. Government purposes.

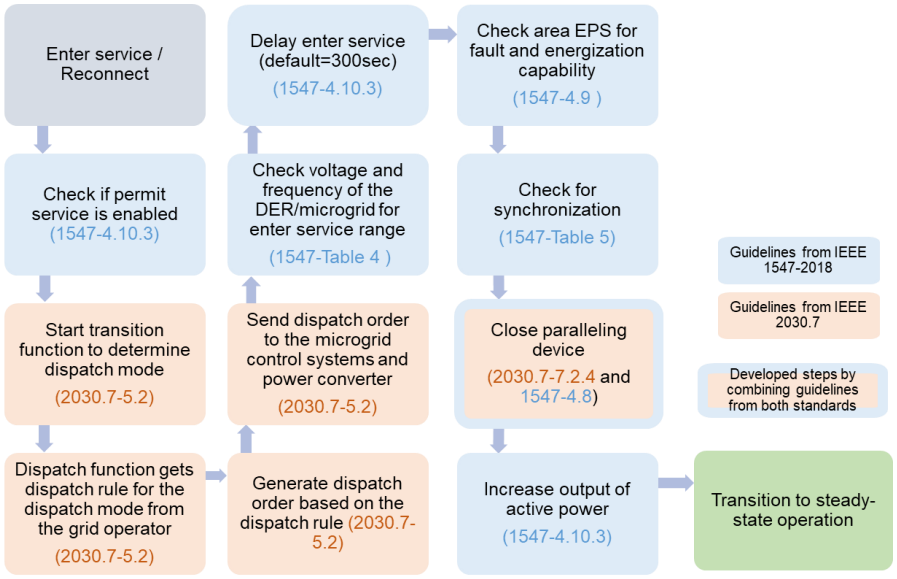

Fig. 2. The control flow diagram for merged IEEE 1547-2018 and IEEE 2030.7 requirements for medium-voltage grid-connected converters to be used for grid interconnects.

II. Grid Controls Applicable Standards and Implementation

In this section, the standards that can be used for the control design of directly connected MVB2B converters are discussed. A use case shows how multiple standards are combined for some functionalities. The gaps in these standards by themselves as applicable for such directly connected MVB2B converters are also identified.

This paper discusses standards that are applicable for the grid-connected operation of a medium-voltage power converter not including communications protocols for this study. The main standards focused on are IEEE 2030.7 and IEEE 1547-2018. The purpose of the IEEE 2030.7 standard is to outline control mechanisms to properly manage and integrate microgrids with the electric power system reliably and seamlessly [13]. It defines the functionalities and requirements of a microgrid controller that monitors the interface between the power grid and the microgrid at the point of connection (POC). Similarly, the IEEE 1547-2018 standard affects the design and capability of the power converters that integrate the DERs to the electric power system [14]. The standard defines frequency and voltage ranges for normal and abnormal operation of DERs. It specifies the grid support functions and the operating regions for the DERs. The advent of medium-voltage SiC switches that have higher voltage blocking capacity, lower loss, and better thermal performance has enabled the design of medium-voltage power converters for grid connection. These converters can be used for myriad grid-connected applications, as shown in Fig. 1. Depending on these applications, the integration and control of such converters can be governed by one or more standards, such as IEEE 2030.7 and IEEE 1547-2018. In the development of different controls for such cases, the appropriate combination of guidelines from both standards must be implemented. One such application for these converters is to be used as grid interconnects between a microgrid and the main power system. The entering service sequence for such use will be based on both IEEE 2030.7 and IEEE 1547-2018 standards, as shown in Fig. 2. The actions shown in the blue boxes (see Fig. 2) are derived from the IEEE 1547-2018 guidelines for entering service command, whereas the actions shown in the orange boxes are derived from steps outlined in IEEE 2030.7. It should be noted that the identification of the sequence of these actions is important for seamless entering of service and for reliable operation of the power grid without causing a transient.

The IEEE 1547-2018 standard outlines ranges for entering service and synchronization. It also specifies the ramp rate for active power after the breaker is closed. It does not specify, however, how to determine the current operating state of the DER and it assumes that the DER will transition to grid-connected mode. It also does not specify the transition function logic that helps determine the operation mode of DERs or to which mode it should transition. On the other hand, the IEEE 2030.7 standard specifies the transition logic for transitioning from islanded mode to grid connected mode. In addition, it provides a flowchart diagram that portrays how the transition knowing the transition mode of the DER helps the dispatch function to fetch the corresponding dispatch rule. Similarly, functions such as power restoration have conflicting requirements from the two standards and need to be identified clearly based on the area power system and grid application of the power converter. The next section presents studies for the grid applications development for directly connected MVB2B power converters.

III. Grid Applications Development

In this section, a series of grid application scenarios are designed to analyze the benefit and impact that a MVB2B converter would bring to the power grid. The objective is to simulate and analyze different grid application use cases, quantify the benefits and impacts of each use case, and then select the grid applications that have more benefits than others. In this paper, a 500 kVA, 13.8 kV three-phase MVB2B converter is added to the IEEE 123-bus test system and the results from the voltage support use cases are presented. All the

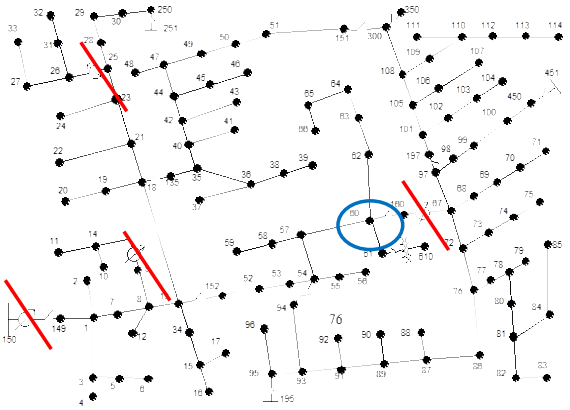

Fig. 3. IEEE 123-bus feeder topology.

simulations performed in these use cases are one-day long with 1-minute resolution. These use cases are targeted at testing and analyzing the voltage support function of the converter.

A. System Setup

In this work, the IEEE 123-bus system is used as the test system, as shown in Fig. 3. This system has 85 load buses, including balanced three-phase load and unbalanced single-phase load. The voltage support and regulation for this system comes from eight devices, including four voltage regulators and four capacitor banks. Instead of simply allocating the substation load onto each load bus with the same load shape inherited from the substation load profile, diversified load profiles are populated to the load buses to guarantee that each load bus has a unique load shape [15]. This helps maintain the load diversity factor of this test system within a reasonable and realistic range, which helps simulate a more realistic environment for the MVB2B converter application testing.

B. Case Study

In this subsection, results from case studies for the voltage support applications of the MVB2B converter are presented. As shown in Fig. 3, a 500 kVA, 13.8 kV, three-phase MVB2B converter is positioned at Bus 60 where the blue circle is placed. Results from two case studies are presented here: high voltage alleviation and real-time voltage regulation. These two use cases are targeted at testing and analyzing the voltage support function of the MVB2B converter. As shown in Fig. 4, it is assumed that for a certain amount of output real power, there is a range of reactive power in which the converter can either generate or absorb reactive power to provide voltage support or voltage regulating service. As shown in Fig. 3, all four regulators are taken out (as shown by the red lines) for the base case and MVB2B converter cases. The capacitor banks are also turned off for all the cases. In order to demonstrate that the voltage regulating function of the converter outperforms the traditional voltage regulators, a test with all the four regulators equipped is done for comparison in the case study of voltage regulation.

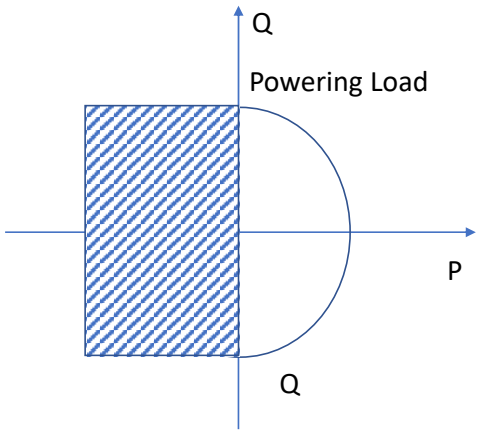

Fig. 4. Model of voltage support function.

Fig. 5 shows the results of the high voltage alleviation case. As the voltage profile rises in the middle of the day (see the red line shown in Fig. 5(a)) because of the solar power back-feeding, it is successfully reduced to approximately 1 per unit (p.u.) with the reactive power absorption function of the converter. Fig. 5(b) shows the reactive power absorption profile for the converter and the upper and lower limits of the reactive power injection/absorption. In this case, it can be observed that approximately half of the absorption capacity is used to reduce the voltage down from 1.02 p.u. to 1.p.u.

Fig. 6 shows the results for a real-time voltage regulation grid application. In Fig. 6 (a), the yellow line represents the basic case with no PV and voltage regulators in the system, the blue line represents the case with 80% penetration of solar generation in the system, the purple line represents the case where voltage regulators are also deployed in the 80% PV penetrated system, and the red line represents the case where the MVB2B converter is used for voltage regulation in the 80% PV penetrated system.

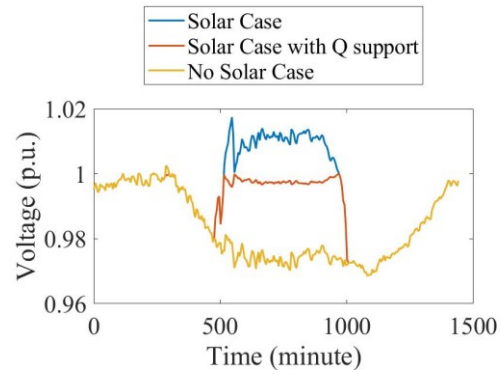

(a)

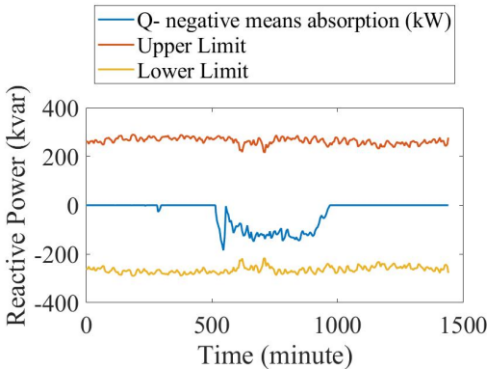

(b)

Fig. 5. Results showing grid application of high voltage alleviation through MVB2B converter.

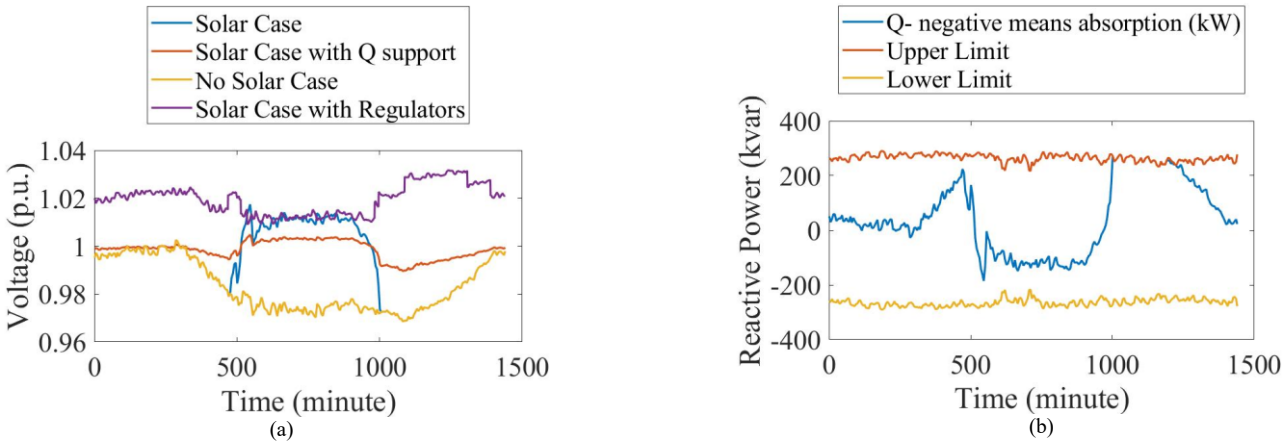

Fig. 6. Results showing grid application of real-time voltage regulation though MVB2B converter.

It can be observed in Fig. 6(a) (see red line) that the voltage profile is successfully maintained at about 1 p.u. with the reactive power injection/generation function of the converter even with a lot of back-feeding solar power during the middle of the day. The purple line in the higher end shows that the voltage profile cannot be regulated well in the case where traditional regulators are working in the system with high solar penetration.

Fig. 6(b) shows the reactive power absorption profile of the converter, where the red and yellow lines represent the upper and lower limit of the reactive power injection/absorption of the converter, respectively. It can be observed that this 500 kVA MVB2B converter is able to absorb the reactive power and regulate the voltage close to 1 p.u. most of the time with little discrepancy. The above voltage support cases demonstrate the voltage regulation capability of the MVB2B converter. These results show that in a system with high PV penetration, a MVB2B converter provides better voltage regulation than traditional voltage regulators. The next section presents the development of control algorithms for these use cases and their evaluation.

IV. Grid Applications Controls and Evaluation

In this section, the control algorithms for the grid applications demonstrated in Section III are developed and evaluated. In order to develop grid-support controls, the MVB2B-connected voltage source converters are modeled, as shown in Fig 7. It should be noted that the actual hardware development for this work uses 10 kV SiC modules, and the topology of the power converter is MVB2B-connected modular multilevel converters. A detailed transient domain switching model of a 500 kVA, three-phase, MVB2B converter (see Fig 7) was developed in PLECS. It was interfaced with Simulink for the control development. The switching frequency used in the simulation is 20 kHz. The developed grid-support controls are volt-watt (VW) for voltage support through active power, frequency-watt (FW) for frequency support through active power, and volt-var (VVAr) for voltage support through reactive power.

A detailed block diagram of the controls for the grid support functions is presented in Fig. 8. Fig. 8 shows the VVAr, VW, and FW implementation in the SimPowerSystems platform. This representation has three parts : the inputs used to obtain the reference points, the controllers used, and the outputs that drive the lower level inverter current control. This control algorithm uses three-phase sinusoidal grid waveforms at point-of-common-coupling (PCC), frequency measurement at PCC, and the apparent power limit on the converter. For voltage regulation, the VVAr and VW controllers generate real and reactive power references, respectively, to control the voltage. The converter uses predefined curves for these functions. It should be noted that during field operation, the converter will be equipped to use the stored default curves or updated curves received in real time from the distribution management system. The three-phase RMS voltage values are calculated and then used to generate references using the default VW and VVAr curves. Since, only the VVAr control sets the reactive power reference, it is directly used to calculate the reference current phase angle (see Fig. 8). The curve used for the VVAr was designed for testing, but it closely resembles the curve from IEEE 1547-2018 [14]. The VVAr-enabled converter injects or absorbs reactive power autonomously to the grid in order to mitigate grid voltage fluctuations based on the grid application studied in the previous section. The real power reference is generated using both the VW and the FW curves. The VW

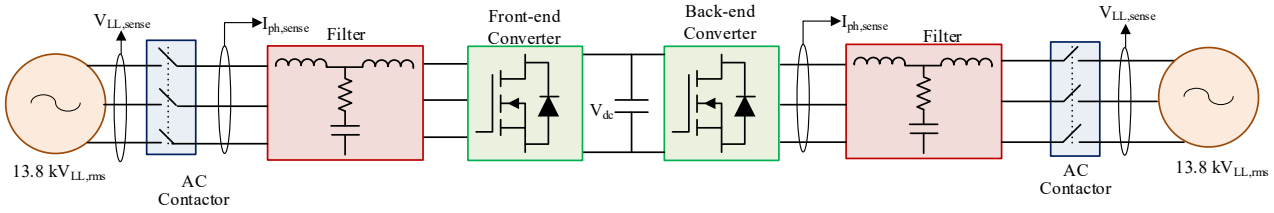

Fig 7. Schematic of the medium-voltage back-to-back converter modeled for controls development.

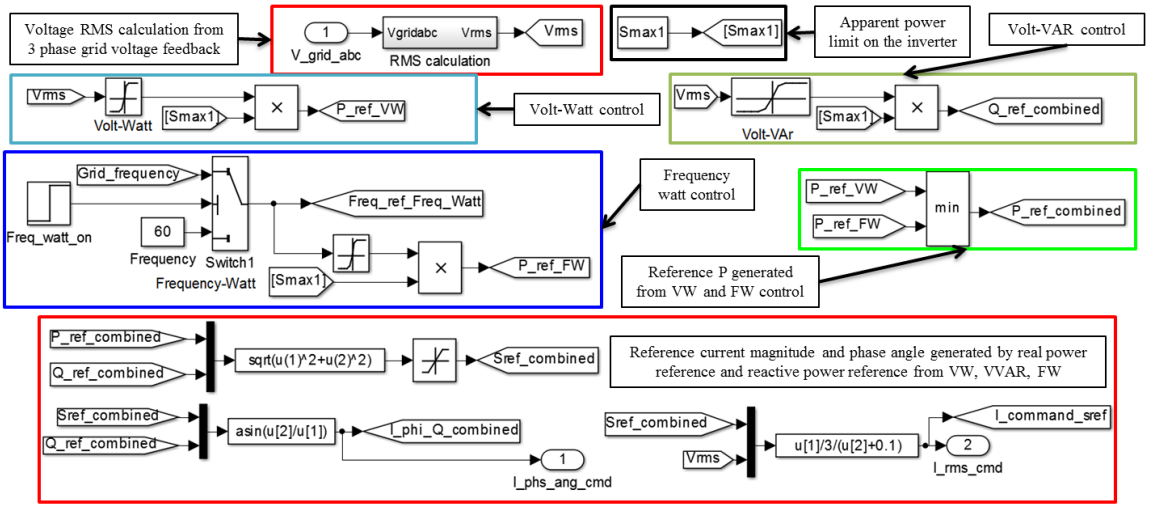

Fig. 8. Developed controller with grid support functionality.

parameters were selected such that after the VVAr control reaches its reactive power absorption limit, the VW curve would start curtailing real power generation. The goal of the FW function is to work along with the VW to generate the real power reference. The curve used for the FW function was also designed to make testing the controllers easier. After two real power references are generated, priority is given to the controller that curtails more. Consider the case when the VW generates a real power reference of 1.0 p.u. and the FW generates a real power reference of 0.5 p.u. In this scenario, priority will be given to the FW power reference, and the inverter will be asked to generate 0.5 p.u. of real power. Finally, a check is made to ensure that the apparent power calculated from the real power and the reactive power references do not exceed the apparent power limit of the inverter. After this check, the current magnitude and the phase angle references are generated for the current control (see Fig. 8).

This control algorithm was implemented on a controller and connected to a CHIL setup for evaluations. The CHIL platform is assembled using a National Instrument's single-board RIO (sbRIO) with General Purpose Inverter Controller mezzanine card (see Fig. 9). The location of different control functions on the controller and the data exchange between different control layers as well as the real-time digital simulator are shown in Fig. 10. The grid support functions – such as VVAr, VW, and FW are programmed in the real-time layer of the controller. The high-speed converter control functions – including the ac current and dc voltage feedback control loops, phase locked loop, and unintentional island-detection algorithms – are coded on the FPGA of the controller. The power converter was implemented on a digital real-time simulator, in this case the Opal-RT OP5607 FPGA expansion unit. The detailed development and evaluation of the CHIL setup is presented in [16].

Fig. 9. Controller used in the CHIL setup.

The first evaluation is for the voltage regulation use case through reactive power support. The VVAr curve used to develop these controls and verify them is shown in Fig. 11 (a). It should be noted that this is only a sample curve closely resembling the curve in IEEE 1547-2018 Category III DER. These controls will help regulate the voltage at the PCC by injecting or absorbing reactive power during any voltage sag or swell event, respectively. The voltage at the terminal of the modeled converter was given step changes, as shown by the blue curve in Fig. 11 (b). The black graph in Fig. 11 (b) shows the reactive power set point with respect to the time calculated using the VVAr curve shown in Fig. 11 (a) for the provided voltage variation. The red graph shown in Fig. 11 (b) is the plot of the measured reactive power at the power converter terminals. It can be observed from Fig. 11 that the measured reactive power closely follows the reference reactive power for the inverter. The developed controls will enable the implementation of the grid application studied in the previous section. These controls will alleviate high voltage and real-time voltage regulation support to the grid.

The second controls evaluated are for the FW grid support function. In this test case, voltage and frequency were controlled

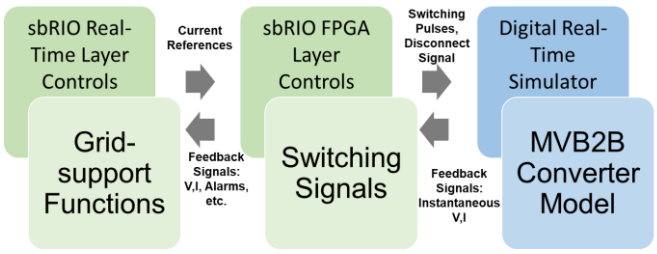

Fig. 10. Block diagram of the CHIL setup.

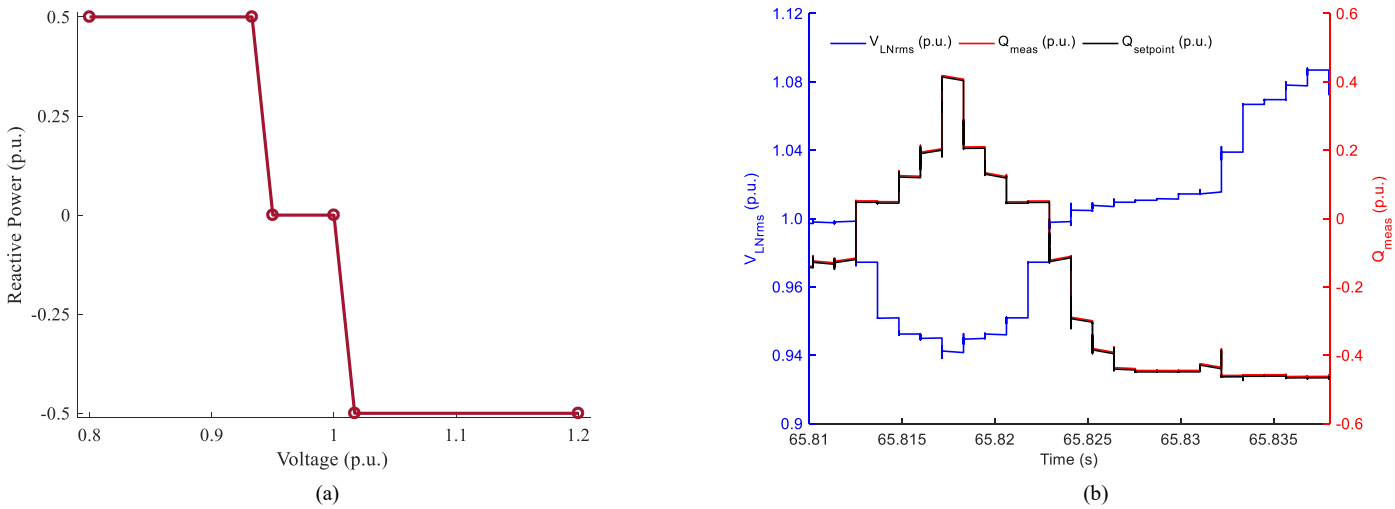

Fig. 11. (a) VVAr curve used for the verification; and (b) CHIL test results showing voltage steps, reactive power set points, and the measured reactive power injected into the grid at the PCC.

in the real-time simulator. Table I summarizes the grid voltage and frequency set points for the test case. The voltage is kept constant at 0.975 p.u. throughout the experiment. The VAr reference for this voltage is zero (see Fig. 11 (a)). The frequency is changed from 60 Hz. to 60.1 Hz. and then back to 60 Hz. At 60.1 Hz., the active power set point is 0.5 p.u. (250 kW) for 60.1 Hz (see Table I). The results obtained from the CHIL evaluations are shown in Fig. 12. The blue curve (see Fig. 12) shows the power grid frequency as observed by the power converter. The green curve shows the real power reference generated using the FW curve. The red curve shows the measured active power injected into the grid at the PCC. It can be observed that the steady-state results match the frequency-watt curve programmed in the controller within the 5% error limit. It should be noted that the ramp observed in the measured active power is caused by the implemented ramp-rate control in the controller. The slope of this change can be modified by modifying the ramp-rate programmed in the controller. The controls developed, evaluated, and validated in this paper include grid support functions, including VVAr, VW, and FW.

TABLE I. SETTINGS FOR TEST CASE USED IN FW VERIFICATION.

Time (s)	V (p.u.)	F step (Hz.)	Watt Reference
0.08	0.975	Steps from 60 to 60.1	Set 1.0 p.u. at 60.0 Hz and 0.5 p.u. at 60.02 Hz
0.3	0.975	Steps from 60.1 to 60	Set 0.5 p.u. at 60.02 Hz and 1.0 p.u. at 60 Hz

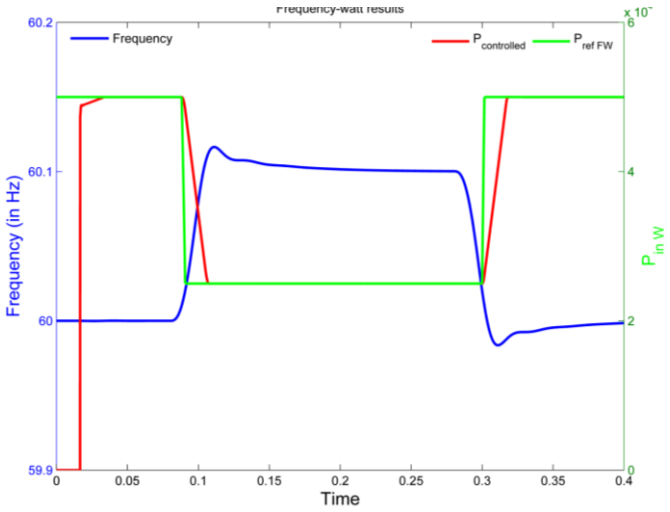

Fig. 12. CHIL test results for FW test case for the grid connected converter.

V. CONCLUSION AND FUTURE WORK

This paper showed the impact of the advent of medium-voltage SiC devices for the power systems. It has been shown how these devices enable myriad direct medium-voltage distribution system connected power converters for grid support applications. The combination of various standards on the control of these power converters has been discussed in this paper. A detailed discussion on how guidelines from standards such as IEEE 2030.7 and IEEE 1547-2018 need to be combined for different operations of a directly grid connected MVB2B power converter has been presented. This has been demonstrated using a use case of entering service. Additionally, a study of grid applications has been presented in this paper. This study quantified and demonstrated how addition of these MVB2B converters to the power grid enables multiple grid support functions. Results from use cases have been presented that demonstrate better voltage regulation in a system with high PV penetration and MVB2B power converters as compared to a high PV penetration system with traditional voltage regulators. Furthermore, control algorithms for the studied grid application of voltage support have been developed for a 500 kW, 13.8 kV back-to-back converter. The developed control algorithms have been implemented on a controller and evaluated on a CHIL setup, in this paper. In the future, other functionalities – such as ride-through, island detection, grid-forming, will be developed and implemented. These controls will also be verified on a SiC-

based MVB2B converter, and the full system will be evaluated for grid benefits in a power-hardware-in-the-loop system.

ACKNOWLEDGMENTS

This work was authored by the National Renewable Energy Laboratory, operated by Alliance for Sustainable Energy, LLC, for the U.S. Department of Energy (DOE) under Contract No. DE-AC36-08GO28308. Funding provided by U.S. Department of Energy Office of Energy Efficiency and Renewable Energy Advanced Manufacturing Office via the GADTAMS Project. The views expressed in the article do not necessarily represent the views of the DOE or the U.S. Government. The U.S. Government retains and the publisher, by accepting the article for publication, acknowledges that the U.S. Government retains a nonexclusive, paid-up, irrevocable, worldwide license to publish or reproduce the published form of this work, or allow others to do so, for U.S. Government purposes.

REFERENCES

[1] T. McNutt "10 kV SiC MOSFET XHV-6 Power Module transitioned to production," https://www.poweramericainstitute.org/wp-content/uploads/2017/02/PowerMerica-Wolfseed-Fayetteville-11Jan17-for-release.pdf last accessed 06/30/2020.

[2] X. Song, C. Peng and A. Q. Huang, "A Medium-Voltage Hybrid DC Circuit Breaker, Part I: Solid-State Main Breaker Based on 15 kV SiC Emitter Turn-OFF Thyristor," in IEEE Journal of Emerging and Selected Topics in Power Electronics, vol. 5, no. 1, pp. 278-288, March 2017.

[3] Z. J. Shen, G. Sabui, Z. Miao and Z. Shuai, "Wide-Bandgap Solid-State Circuit Breakers for DC Power Systems: Device and Circuit Considerations," in IEEE Transactions on Electron Devices, vol. 62, no. 2, pp. 294-300, Feb. 2015, doi: 10.1109/TED.2014.2384204.

[4] A. Abramovitz, K. M. Smedley, "Survey of solid-state fault current limiters," IEEE Trans. Power Electron., vol. 27, no. 6, pp. 2770-2782, Jun, 2012.

[5] M. Montero, E. Cadaval, F. Gonzalez, "Comparison of control strategies for shunt active power filters in three-phase four-wire systems," IEEE Trans. Power Electron., vol. 22, no. 1, pp. 229-236, Jan. 2007.

[6] S. B. Kjaer, J. K. Pedersen, and F. Blaabjerg, "A review of single-phase grid-connected inverters for photovoltaic modules," IEEE Trans. Ind. Appl., vol. 41, pp. 1292-1306, Sep./Oct. 2005.

[7] F. Blaabjerg, M. Liserre, and K. Ma, "Power electronics converters for wind turbine systems," IEEE Trans. Ind. Appl., vol. 48, no. 2, pp. 708-719, Mar./Apr. 2012.

[8] J. Carrasco, L. Franquelo, J. Bialasiewicz, "Power-electronic systems for the grid integration of renewable energy sources: a survey," IEEE Trans. Ind. Electron., vol. 53, no. 4, pp. 1002-1016, Apr. 2006.

[9] B. Kroposki et al., "Achieving a 100% renewable grid: Operating electric power systems with extremely high levels of variable renewable energy," IEEE Power Energy Mag., vol. 15, no. 2, pp. 61–73, Mar./Apr. 2017.

[10] H. Choi, M. Ciobotaru, M. Jang, and V. G. Agelidis, "Performance of medium-voltage dc-bus PV system architecture utilizing high-gain dc– dc converter," IEEE Trans. Sustain. Energy, vol. 6, no. 2, pp. 464–473, Apr. 2015.

[11] T. Kerekes, E. Koutroulis, D. Sera, R. Teodorescu, and M. Katsanevakis, "An optimization method for designing large PV plants," IEEE J. Photovolt., vol. 3, no. 2, pp. 814–822, Apr. 2013.

[12] B. B. Johnson, S. V. Dhople, A. O. Hamadeh, and P. T. Krein, "Synchronization of parallel single-phase inverters with virtual oscillator control," IEEE Trans. Power Electron., vol. 29, no. 11, pp. 6124–6138, Nov. 2014.

[13] IEEE, "IEEE 2030.7-2017 - IEEE Standard for the Specification of Microgrid Controllers," New York, 2017.

[14] IEEE Standard for Interconnection and Interoperability of Distributed Energy Resources with Associated Electric Power Systems Interfaces," in *IEEE Std 1547-2018 (Revision of IEEE Std 1547-2003)*, vol., no., pp.1-138, 6 April 2018

[15] X. Zhu and B. Mather, "Data-Driven Distribution System Load Modeling for Quasi-Static Time-Series Simulation," in *IEEE Transactions on Smart Grid*, vol. 11, no. 2, pp. 1556-1565, March 2020.

[16] A. Singh and K. Prabakar, "Controller-Hardware-in-the-Loop Testbed for Fast-Switching SiC-Based 50-kW PV Inverter," *IECON 2018 - 44th Annual Conference of the IEEE Industrial Electronics Society*, Washington, DC, 2018, pp. 1109-1115